

Tension-torsion in a circular bar of elastic, linear-strain-hardening and rate-sensitive material

S. A. MEGUID (CRANFIELD)

A NUMERICAL solution of the elastic-linear strain hardening behaviour of a solid cylindrical bar, made of a homogeneous, isotropic and rate-dependent material, subjected to proportional and non-proportional deformation programmes of twist and stretch, without unloading or reversed loading, is presented. In this investigation the material is assumed to yield according to the von Mises criterion and then to follow a rate-dependent post-yield constitutive law of the Perzyna type. The material is also assumed to work-harden isotropically and this hardening is unaffected by the rate of straining. The analysis is applicable in the medium rate range where inertia effects are negligible. Several different deformation paths are investigated and the resulting stresses and load-torque trajectories are calculated. For each deformation path, numerical solution of the governing system of quasi-linear partial differential equations gave the loading trajectories and the radial variations of the stress field at selected times. Comparison with predictions of a rate-dependent but non-work-hardening material is also made. The load trajectories computed for the different rectilinear straining paths show that, for a considerable length of the post-yield deformation path, the slope of the trajectory is essentially equal to that which would correspond to elastic straining. This slope changes, however, before the trajectory crosses the limiting state locus of the non-work-hardening material.

Przedstawiono rozwiązanie numeryczne dla pręta o pełnym przekroju kołowym wykonanego z materiału sprężysto-plastycznego o liniowym wzmocnieniu. Materiał pręta jest jednorodny, izotropowy i wrażliwy na prędkość odkształcenia, a programy obciążenia siłami rozciągającymi i momentami skręcającymi są proporcjonalne lub nieproporcjonalne i nie zawierają odciążania lub obciążania przeciwnego. W rozważaniach przyjęto, że materiał płynie zgodnie z kryterium von Misesa, a następnie podlega prawu konstytutywnemu typu Perzyna dla materiałów wrażliwych na prędkość odkształcenia. Założono również izotropowe wzmocnienie materiału niezależne od prędkości odkształcenia. Analiza stosuje się do przypadków o umiarkowanej prędkości odkształcenia, w których zaniedbać można wpływ członów inercyjnych. Rozpatrzono kilka różnych dróg obciążenia i obliczono odpowiadające im trajektorie sił i momentów. Dla każdej drogi obciążenia rozwiązanie numeryczne odpowiedniego układu quasi-liniowych, cząstkowych równań różniczkowych podaje trajektorie obciążeń oraz promieniowy rozkład pola naprężenia dla wybranych wartości czasu. Wyniki porównano z danymi dotyczącymi materiałów wrażliwych na prędkość odkształcenia bez wzmocnienia. Trajektorie obciążeń obliczone dla różnych prostoliniowych dróg odkształcenia pokazują, że przy dostatecznie długich drogach deformacji po uplastycznieniu, nachylenie trajektorii jest w zasadzie takie samo jak w przypadku odkształcenia sprężystego. Nachylenie to zmienia się jednak przed przecięciem przez trajektorię miejsca geometrycznego stanów granicznych dla ciała bez wzmocnienia.

Представлено численное решение для стержня с полным круговым сечением, изготовленного из упруго-пластического материала с линейным упрочнением. Материал стержня однородный, изотропный и чувствителен на скорость деформации, а программы нагружения растягивающими силами и скручивающими моментами пропорциональны или непропорциональны и не содержат разгрузки или противоположного нагружения. В рассуждениях принимается, что материал течет согласно критерию Мизеса, а затем подлжит определяющему закону типа Перзина для материалов чувствительных на скорость деформации. Предложено тоже изотропное упрочнение материала независящие от скорости деформации. Анализ применяется для случаев с умеренными скоростями деформации, в которых можно пренебречь влиянием инертных членов. Рассмотрено несколько разных путей нагружения и вычислены отвечающие им траектории сил и моментов. Для каждого пути нагружения численное решение отвечающей системы квазилинейных дифференциальных уравнений в частных производных дает траектории

нагружений и радиальное распределение поля напряжений для избранных моментов времени. Результаты сравнены с данными, касающимися материалов чувствительных на скорость деформации без упрочнения. Траектории нагружений, вычисленные для разных прямолинейных путей деформации, показывают, что при достаточно длинных путях деформации после перехода в пластическое состояние, наклон траектории в принципе такой же сам, как в случае упругой деформации. Этот наклон изменяется однако перед пересечением через траекторию геометрического места предельных состояний для тела без упрочнения.

1. Introduction

IN TWO recent publications, MEGUID and CAMPBELL [1] and MEGUID, CAMPBELL and MALVERN [2] examined the effect of the deformation path upon the resulting stresses and loads for a rate sensitive but non-work-hardening material. In these two articles the material behaviour was assumed to follow Perzyna's rate-dependent constitutive laws and to yield according to the von Mises yield criterion. The radial variations of the stresses and loads were determined numerically using a finite-difference scheme. Analytical expressions for limit state stresses and loads for a rigid-perfectly-plastic and rate-sensitive material were determined and discussed in terms of extension/twist ratio, strain rate and some characteristic constants used to define the material.

In this paper an attempt is made to extend the previous MEGUID *et al.* [1] and [2] work to materials that strain harden. The hardening model assumed in this article is a simple one. It is isotropic, rate-insensitive and linear; the linearity is between the equivalent stress and equivalent strain (see Eq. (2.5)). As in [1] and [2], the effects of post-yield deformation upon the radial variations of the stresses and loads as a result of following different straining routes are discussed. These radial variations of the stresses and loads are then compared with the previous results obtained from considering a rate-sensitive but non-work-hardening material behaviour (described in details in [1] and [2]).

2. Theoretical analysis

The details of the analytical and numerical procedures adopted in this investigation are described in MEGUID and CAMPBELL [1]. We present here only a summary of the techniques used, together with necessary alterations needed to accommodate the linear-strain-hardening effects.

The theoretical analysis employs a cylindrical coordinate system (r , θ and z) with the z -axis taken to coincide with the bar axis. Because of axial symmetry displacements, velocities, strains, strain rates and stresses must be independent of the circumferential variable θ . Since the bar cross-section is uniform along the axial direction, the compatibility condition reduces to

$$(2.1) \quad \frac{\partial e_r}{\partial r} + 2 \frac{\partial e_\theta}{\partial r} = \frac{e_r - e_\theta}{r},$$

where e_r and e_θ are the deviatoric strains in the radial and tangential directions, respectively.

Equilibrium of the bar in the radial direction gives

$$(2.2) \quad \frac{\partial \sigma_r}{\partial r} + \frac{\sigma_r - \sigma_\theta}{r} = 0.$$

The other two equilibrium equations are identically satisfied.

In problems involving a multiaxial state of stress it is necessary to have a general relationship between the components of the stress and strain rate tensors. In the present study we adopt PERZYNA'S [3, 4] incremental post-yield constitutive laws which may be expressed as the following relation between the deviatoric strain rate tensor \dot{e}_{ij} and the deviatoric stress tensor s_{ij} :

$$(2.3) \quad \frac{\partial e_{ij}}{\partial t} = \frac{1}{2G} \frac{\partial s_{ij}}{\partial t} + \frac{3}{2} \frac{s_{ij}}{\bar{\sigma}} \langle \phi(\bar{\sigma}, \bar{\varepsilon}) \rangle,$$

where $\phi(\bar{\sigma}, \bar{\varepsilon})$ is a plastic stress-strain rate function⁽¹⁾. Here G is the shear modulus and $\bar{\sigma}$ is the von Mises equivalent stress defined as $\bar{\sigma} = \left(\frac{3}{2} s_{ij} s_{ij} \right)^{1/2}$. In the present application of the theory the following modified form of ϕ , suggested by PERZYNA [3, 4] as a generalisation of the uniaxial formulation of COWPER and SYMONDS [5], was used, i.e.

$$(2.4) \quad \phi(\bar{\sigma}) = C \left(\frac{\bar{\sigma}}{\sigma(\bar{\varepsilon})} - 1 \right)^\delta,$$

where $\sigma(\bar{\varepsilon})$ is the instantaneous quasi-static yield stress, and for a linear-strain-hardening material it may be expressed as a linear function of the quasi-static equivalent strain $\bar{\varepsilon}$, viz.

$$(2.5) \quad \sigma(\bar{\varepsilon}) = (1 - \alpha)\sigma_0 + \alpha E \bar{\varepsilon} \quad \text{for} \quad \bar{\varepsilon} > \varepsilon_0.$$

Here $\bar{\varepsilon}$ is the von Mises equivalent strain defined as $\bar{\varepsilon} = \int d\bar{\varepsilon} = \int \left(\frac{2}{3} d\bar{\varepsilon}_{ij} d\bar{\varepsilon}_{ij} \right)^{1/2}$, α is the ratio between the plastic and elastic moduli for a bilinear material, σ_0 is the initial quasi-static yield stress and E is the Young's modulus.

The numerical analysis may be simplified by normalising the normal stresses and strains by their initial quasi-static yield values σ_0 and ε_0 and the shear stresses and strains by k_0 and γ_0 . Normalised quantities are denoted by boldface type, e.g. $\boldsymbol{\sigma}_z = \sigma_z/\sigma_0$, $\boldsymbol{\sigma} = \bar{\sigma}/\sigma_0$ and $\boldsymbol{\gamma} = \gamma/\gamma_0$. Let us also introduce a non-dimensional time parameter λ which is defined by $\lambda = Ct$, where C is a material constant defined in Eq. (2.4), and a non-dimensional radial coordinate defined by $\mathbf{r} = r/R$, where R is the bar radius.

If Eqs. (2.3) and (2.4) are combined together, the result in a normalised form is as follows:

$$(2.6) \quad \frac{\partial \mathbf{e}_{ij}}{\partial \lambda} = (1 + \nu) \frac{\partial \mathbf{s}_{ij}}{\partial \lambda} + \frac{3}{2} \frac{\mathbf{s}_{ij}}{\boldsymbol{\sigma}} \left(\frac{\boldsymbol{\sigma}}{\boldsymbol{\sigma}(\bar{\boldsymbol{\varepsilon}})} - 1 \right)^\delta \frac{E}{\sigma_0}.$$

Equation (2.6) together with the non-dimensional form of the compatibility condition (2.1) and equilibrium equation (2.2) form a set of quasi-linear partial differential equations of the first order which may be integrated numerically, using a finite difference scheme,

⁽¹⁾ The symbol $\langle \phi \rangle$ represents ϕ if $\phi > 0$, zero if $\phi \leq 0$.

along the characteristics $r = \text{constant}$ and $\lambda = \text{constant}$ from known boundary and initial conditions. Calculations proceeded by forward difference from the bar centre. In each time increment, $d\lambda$, it was necessary to solve six nonlinear simultaneous equations in the unknown variables e_r , e_θ , s_r , s_θ , τ , and $\bar{\sigma}$.

Numerical solution of the governing equations gave the deviatoric stresses and strains as functions of r and λ . The conventional stresses and strains were then calculated from the elastic compressibility condition and the known ϵ_z and γ at selected times λ . Finally, the normalised axial load P and torque T acting on the bar were calculated by approximate numerical integration⁽²⁾.

If the rate-dependent material investigated is of the rigid-perfectly-plastic type, a closed form solution of the stresses and loads may be obtained. These solutions are referred to in this article as the limit state. The details of the calculations of the normalised limit state load P^* and torque T^* can be found in MEGUID and CAMPBELL [1].

3. Analysis of results

In order to examine the hardening effect upon the resulting stresses and loads, it was felt necessary to follow the same proportional and non-proportional deformation paths investigated earlier by MEGUID and CAMPBELL [1] and recently by MEGUID, CAMPBELL and MALVERN [2], but for a non-work-hardening material. This enables us to compare the stress and load fields.

Four types of deformation path were investigated, as follows:

1) The bar is extended quasi-statically to the initial yield point ($\epsilon_z = 1$); the extension is then held constant while the angle of twist is increased at a uniform rate giving a maximum equivalent strain rate

$$\eta = \left(\frac{2}{3} \dot{\epsilon}_{ij} \dot{\epsilon}_{ij} \right)^{1/2} = 0.02C.$$

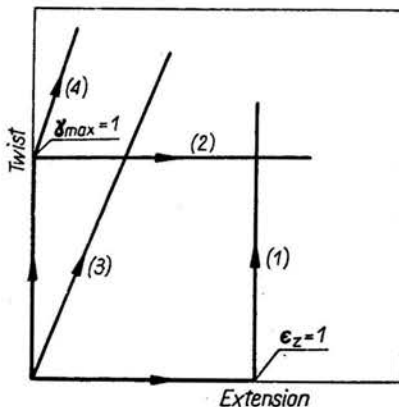


FIG. 1. Types of deformation paths investigated (see Table 1 for details).

⁽²⁾ P and T are normalised by their initial quasi-state yield values in simple tension and pure shear, respectively.

2) The bar is twisted quasi-statically until it yields at its surface ($\gamma = 1$ at $r = 1$); the angle of twist is then held constant while the bar is extended at a constant rate corresponding to $\eta = 0.02C$.

3) The bar is simultaneously extended and twisted so that $(\dot{\gamma}/\dot{\epsilon}_z)$ is constant and the equivalent strain rate at the bar surface is again $0.02C$.

4) The bar is twisted quasi-statically to the initial yield point, as in 2), and then simultaneously extended and twisted as in 23).

Figure 1 indicates these four types of deformation path, and Table 1 gives the details of the particular paths chosen, together with the P^* and T^* values as calculated from the limit state closed form solutions corresponding to the rigid-perfectly-plastic and rate-sensitive material.

Table 1. Data for the proportional and non-proportional deformation paths investigated. (Maximum strain rate $\eta = 0.02C$ for all paths)

Path No.	Type of path	Angle of load trajectory for elastic straining	Initial Yield		Limit State ⁽³⁾	
			P_0	T_0	P^*	T^*
(1)	Extension, then twisting	90°	1	0	0	1.905
(2)	Twisting, then extension	0°	0	1	1.457	0
(3)	Proportional straining	60°	0.5	0.866	1.03	1.388
(4)	Twisting, then proportional straining	71.6°	0	1	0.954	1.479

⁽³⁾ These limit state loads and torques correspond to a material which is rigid perfectly plastic and rate-sensitive.

The numerical calculations were carried out using the following values for the material constants:

$$\sigma_0/E = 10^{-3}, \quad \nu = 0.28, \quad C = 40 \text{ s}^{-1}, \quad \delta = 5 \quad \text{and} \quad \alpha = 0.05.$$

These are typical of the experimental data for mild steel, the values for C and δ being those determined by BODNER and SYMONDS [6] from the results of MANJOINE [7].

For all the straining paths considered, the computed normalised radial and transverse stresses σ_r and σ_θ were very small compared with the main active stresses σ_z and τ and can be ignored for all practical applications. A similar result has been obtained by MEGUID and CAMPBELL [1] for a rate-sensitive but non-work-hardening material and by BROOKS [8] in an earlier work for a work-hardening but rate-insensitive material behaviour.

The general trend of the stresses and load resulting from following the different deformation paths are similar. Therefore, it was felt unnecessary to investigate all the four straining paths. In this article only path (2) will be considered in some details. This will be followed by a summary of the four load trajectories.

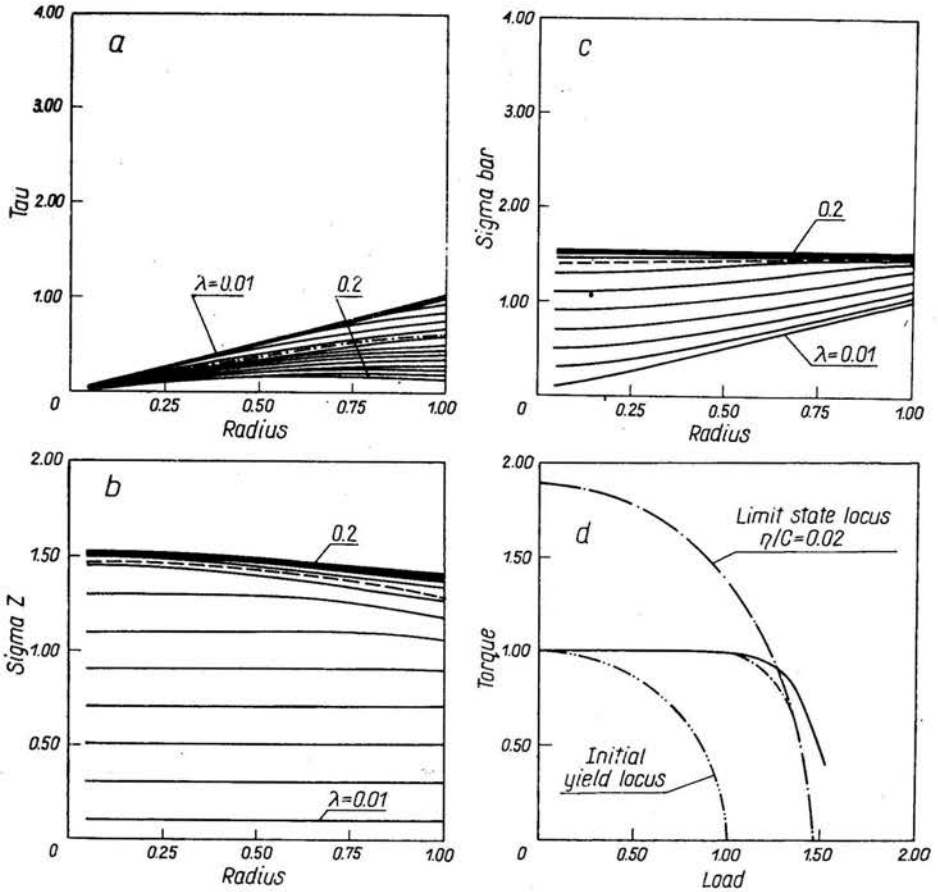


FIG. 2. Normalised results for path (2): (a) shear stress, (b) axial stress, (c) equivalent stress and (d) loading trajectory. Perforated curves represent the solution for a rate-sensitive but non-work-hardening material.

Figures 2 show the variation in the shear stress τ , axial stress σ_z and equivalent stress $\bar{\sigma}$ for path (2), and 4(d) shows the corresponding load trajectory in the (P, T) plane. For constant quasi-static twisting of the bar, the shear stress distribution is linear (zero at the bar centre and unity at the bar outer boundary). As the deformation continues and λ increases, the axial stresses σ_z start to develop while the linear distribution of the shear stresses remains unchanged. As λ continues to increase, the shear stresses start to decrease at and near the bar outer boundary and the axial stresses continue to increase. The increase in σ_z develops faster than the decrease in τ , such that the equivalent stress $\bar{\sigma}$ increases from its linear distribution corresponding to the quasi-static twisting of the bar towards the over-stress value relating to what is known as the limiting state condition for a rigid-perfectly-plastic and rate-sensitive material at the given equivalent strain rate η . Although the general shapes of the stress distributions (axial and shear) are similar to those determined from the non-work-hardening model [1], the stress levels in this study are in general higher. Note that the deformation time is double that of the early investigations [1, 2].

From comparison of the twist-extension and the normalised torque-load plot, it appears that during the early stages of post-yield deformation the two paths are similar. However, when \mathbf{P} exceeds about 1, τ decreases significantly while σ_z continues to increase with increasing time λ . This results in a decrease in the torque \mathbf{T} and an increase in the load \mathbf{P} . As the deformation continues, the load trajectory crosses what is known as the limit state locus for a rigid perfectly plastic and rate-sensitive material behaviour. The perforated curve shows the elasto-plastic solution for a rate-sensitive but non-work-hardening material together with the limit state locus for $\eta = 0.02 C$.

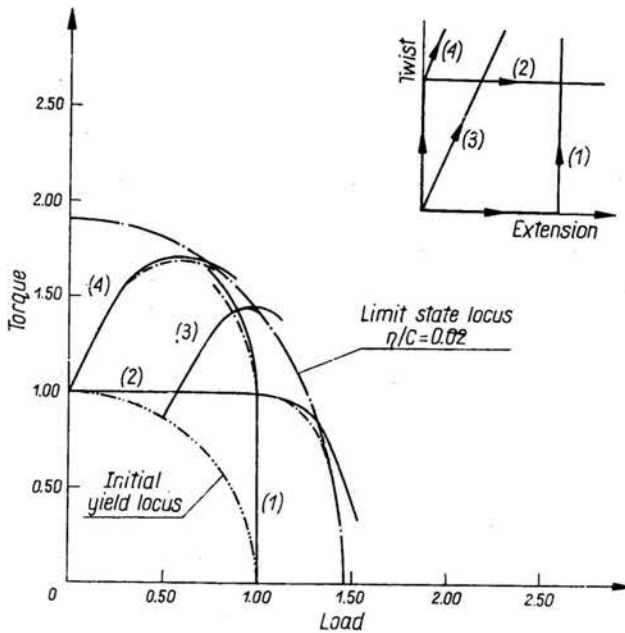


FIG. 3. Normalised load-torque trajectories for the four prescribed deformation paths. Perforated curves represent the solution for a rate-sensitive but non-work-hardening material.

Figure 3 sums up the load trajectories resulting from following the different deformation paths investigated. It is clear that, during the early stages of post-yield deformation, features similar to those presented earlier for a rate-sensitive but non-work-hardening material are noticed. The load trajectories computed for the different deformation paths show that during these early stages of post-yield deformation the slope of the trajectory is essentially equal to that which would correspond to elastic straining. After a considerable change has occurred in torque (as in path (1)) or load (as in path (2)) or both (as in paths (3) and (4)), the slope of the trajectory changes as the load and torque approach the limit state locus which corresponds to a rigid-perfectly-plastic and rate-sensitive material behaviour. As the deformation continues, the trajectories of the hardening material cross this limit state locus of the non-hardening material.

4. Conclusions

The problem of combined extension and twisting of a solid circular bar of rate-sensitive and linear-strain-hardening material has been solved numerically for various proportional and non-proportional straining paths.

The computed normalised radial and circumferential stresses were found to be very small compared to the axial and shear stresses and can be ignored for all practical applications. The distribution of these latter normalised stresses and the load trajectory in normalised tension-torque space have been determined and plotted for four particular straining paths. For these calculations the material behaviour was taken to be governed by Perzyna's rate-dependent constitutive relation, the yield criterion being that of von Mises and the numerical constants appropriate to mild steel. The linear-work-hardening was assumed to be isotropic and rate-insensitive.

Features similar to those presented in an early investigation by MEGUID and CAMPBELL for a rate sensitive but non-work hardening material are noticed. The load trajectories computed for rectilinear straining paths show that during the early stages of post-yield deformation the slope of the trajectory is essentially equal to that which would correspond to elastic straining. After a considerable change has occurred in load or torque or both, the slope of the trajectory changes as the load and torque approach what is known as the limit state locus for a rigid-perfectly-plastic and rate-sensitive material. As the deformation continues the load trajectory crosses this limit state locus.

Acknowledgement

The author acknowledges the helpful discussions with Professor L. E. MALVERN of the Engineering Sciences Department, University of Florida, Gainesville, USA, during the course of this work.

References

1. S. A. MEGUID and J. D. CAMPBELL, *Elastic-plastic tension-torsion in a circular bar of rate-sensitive material*, *J. Appl. Mech.*, **46**, 311-316, 1979.
2. S. A. MEGUID, J. D. CAMPBELL and L. E. MALVERN, *On the elastic-viscoplastic proportional combined twist and stretch of a circular bar of rate-sensitive material*, *J. Mech. Phys. Solids*, **27**, 331-343, 1979.
3. P. PERZYNA, *Fundamental problems in viscoplasticity*, *Advances in Applied Mechanics*, ed. G. KUERTI, **9**, 243-377, Academic Press, New York 1966.
4. P. PERZYNA, *Thermodynamic theory of viscoplasticity*, *Advances in Applied Mechanics*, ed. C. S. YIH, **11**, 313-354, Academic Press, New York 1971.
5. G. R. COWPER and P. S. SYMONDS, *Strain hardening and strain rate effects in the impact loading of cantilever beams*, Tech. Report No. 28, from Brown University to the Office of Naval Research under contract Nonr-562(10), 1957.
6. S. R. BODNER and P. S. SYMONDS, *Experimental and theoretical investigation of the plastic deformation of cantilever beams subjected to impulsive loading*, *J. Appl. Mech.*, **29**, 719-728, 1962.

7. M. J. MANJOINE, *Influence of rate of strain and temperature on yield stresses of mild steel*, J. Appl. Mech., **11**, Trans. ASME, **66**, 211-218, 1944.
8. D. S. BROOKS, *The elasto-plastic behaviour of a circular bar loaded by axial force and torque in the strain hardening range*, Int. J. Mech. Sciences, **11**, 75-85, 1969.

APPLIED MECHANICS GROUP
SCHOOL OF MECHANICAL ENGINEERING
CRANFIELD INSTITUTE OF TECHNOLOGY
CRANFIELD, BEDFORD, U. K.

Received August 17, 1979.
